Journal of Computational and Applied Mathematics 313 (2017) 202–217

Contents lists available at ScienceDirect

Journal of Computational and Applied Mathematics

journal homepage: www.elsevier.com/locate/cam

A weak Local Linearization scheme for stochastic differential equations with multiplicative noise

J.C. Jimenez [a,*], C. Mora [b], M. Selva [c]

[a] Instituto de Cibernética, Matemática y Física, La Habana, Cuba

[b] Departamento de Ingeniería Matemática and CI²MA, Universidad de Concepción, Chile

[c] Departamento de Ingenería Matemática, Universidad de Concepción, Chile

ARTICLE INFO

Article history:
Received 21 June 2015
Received in revised form 21 July 2016

MSC:
65C30
60H10
60H35

Keywords:
Stochastic differential equation
Mean-square stability
Weak convergence
Local Linearization scheme

ABSTRACT

In this paper, a weak Local Linearization scheme for Stochastic Differential Equations (SDEs) with multiplicative noise is introduced. First, for a time discretization, the solution of the SDE is locally approximated by the solution of the piecewise linear SDE that results from the Local Linearization strategy. The weak numerical scheme is then defined as a sequence of random vectors whose first moments coincide with those of the piecewise linear SDE on the time discretization. The scheme is explicit, preserves the first two moments of the solution of SDEs with linear drift and diffusion coefficients in state and time, and inherits the mean-square stability or instability that such solution may have. The rate of convergence is derived and numerical simulations are presented for illustrating the performance of the scheme.

1. Introduction

During 30 years the class of Local Linearization integrators has been developed for different types of deterministic and random differential equations. The essential principle of such integration methods is the piecewise linearization of the given differential equation to obtain consecutive linear equations that are explicitly solved at each time step. This general approach has worked well for the classes of ordinary, delay, random and stochastic differential equations. Key element of such success is the use of explicit solutions or suitable approximations for the resulting linear differential equations. Precisely, the absence of explicit solution or adequate approximation for linear Stochastic Differential Equations (SDEs) with multiplicative noise is the main reason of the limited application of the Local Linearization approach to nonlinear SDEs with multiplicative noise. For these equations, the available Local Linearization integrators are of two types: those introduced in [1] for scalar equations and those considered in [2–4]. The former uses the explicit solution of the scalar linear equations with multiplicative noise, while the latter employs the solution of the linear equation with additive noise that locally approximates the nonlinear equation.

Directly related to the development of the Local Linearization integrators is the concept of Local Linear approximations (see, e.g., [5–7]). These approximations to the solution of the differential equations are defined as the continuous time solution of the piecewise linear equations associated to the Local Linearization method. These continuous approximations have played a fundamental role for studying the convergence, stability and dynamics of the Local Linearization integrators for all the classes of differential equations mentioned above with the exception of the SDEs with multiplicative noise. For

* Corresponding author.
E-mail addresses: jcarlos@icimaf.cu (J.C. Jimenez), cmora@ing-mat.udec.cl (C. Mora), selva@ing-mat.udec.cl (M. Selva).

http://dx.doi.org/10.1016/j.cam.2016.09.013
0377-0427/

this last class of equations, the Local Linear approximations have only been used for constructing piecewise approximations to the mean and variance of the states in the framework of continuous–discrete filtering problems (see [7]).

The purpose of this work is to construct a weak Local Linearization integrator for SDEs with multiplicative noise based on suitable weak approximation to the solution of piecewise linear SDEs with multiplicative noise. For this, we cross two ideas: (1) as in [7], the use of the Local Linear approximations for obtaining piecewise approximations to the mean and variance of the SDEs with multiplicative noise; and (2) as in [8], at each integration step, the generation of a random vector with the mean and variance of the Local Linear approximation at this integration time. For implementing this, new formulas recently obtained in [9] for the mean and variance of the solution of linear SDEs with multiplicative noise are used, which are computationally more efficient than those formerly proposed in [10,7]. Notice that this integration approach is conceptually different to that usually employed for designing weak integrators for SDEs. Typically, these integrators are derived from a truncated Ito–Taylor expansion of the equation's solution at each integration step, and include the generation of random variables with moments equal to those of the involved multiple Ito integrals [11,12].

The paper is organized as follows. After some basic notations in Section 2, the new Local Linearization integrator is introduced in Section 3. Its rate of convergence is derived in Section 4 and, in the last section, numerical simulations are presented in order to illustrate the performance of the numerical integrator.

2. Basic notations

Let us consider the SDE with multiplicative noise

$$X_t = X_{t_0} + \int_{t_0}^{t} f(s, X_s)\, ds + \sum_{k=1}^{m} \int_{t_0}^{t} g^k(s, X_s)\, dW_s^k, \quad \forall t \in [t_0, T], \tag{1}$$

where $f, g^k : [t_0, T] \times \mathbb{R}^d \to \mathbb{R}^d$ are smooth functions for all $k = 1, \ldots, m$, $W^1, \ldots, W^m$ are independent Wiener processes on a filtered complete probability space $\left(\Omega, \mathfrak{F}, (\mathfrak{F}_t)_{t \geq t_0}, \mathbb{P}\right)$, and X_t is an adapted $\mathbb{R}^d$-valued stochastic process. In addition, let us assume the usual conditions for the existence and uniqueness of a weak solution of (1) with bounded moments (see, e.g., [11]).

Throughout this paper, we consider the time discretization $t_0 = \tau_0 < \tau_1 < \cdots < \tau_N = T$ with $\tau_{n+1} - \tau_n \leq \Delta$ for all $n = 0, \ldots, N-1$ and $\Delta > 0$. We use the same symbol $K(\cdot)$ (resp., K) for different positive increasing functions (resp., positive real numbers) having the common property to be independent of $(\tau_k)_{k=0,\ldots,N}$. Moreover, $A^\top$ stands for the transpose of the matrix A, and $|\cdot|$ denotes the Euclidean norm for vectors. $C_p^\ell\left(\mathbb{R}^d, \mathbb{R}\right)$ denotes the collection of all ℓ-times continuously differentiable functions $g : \mathbb{R}^d \to \mathbb{R}$ such that g and all its partial derivatives of orders $1, 2, \ldots, \ell$ have at most polynomial growth. A random variable η with mean $\overline{\eta}$ will be called symmetric around the mean $\overline{\eta}$ if $\eta - \overline{\eta}$ and $-(\eta - \overline{\eta})$ have the same distribution.

3. Numerical method

Suppose that $z_n \approx X_{\tau_n}$ with $n = 0, \ldots, N-1$. Set $g^0 = f$. Taking the first-order Taylor expansion of g^k yields

$$g^k(t, x) \approx g^k(\tau_n, z_n) + \frac{\partial g^k}{\partial x}(\tau_n, z_n)(x - z_n) + \frac{\partial g^k}{\partial t}(\tau_n, z_n)(t - \tau_n)$$

whenever $x \approx z_n$ and $t \approx \tau_n$ for all $k = 0, \ldots, m$. Therefore

$$X_t \approx z_n + \sum_{k=0}^{m} \int_{\tau_n}^{t} \left(B_n^k X_s + b_n^k(s)\right) dW_s^k \quad \forall t \in [\tau_n, \tau_{n+1}],$$

with $W_s^0 = s$, $B_n^k = \frac{\partial g^k}{\partial x}(\tau_n, z_n)$ and

$$b_n^k(s) = g^k(\tau_n, z_n) - \frac{\partial g^k}{\partial x}(\tau_n, z_n)\, z_n + \frac{\partial g^k}{\partial t}(\tau_n, z_n)(s - \tau_n). \tag{2}$$

This follows that, for all $t \in [\tau_n, \tau_{n+1}]$, X_t can be approximated by

$$Y_t = z_n + \sum_{k=0}^{m} \int_{\tau_n}^{t} \left(B_n^k Y_s + b_n^k(s)\right) dW_s^k, \quad \forall t \in [\tau_n, \tau_{n+1}], \tag{3}$$

which is the first order Local Linear approximation of X_t used in [7]. From (3) we have that $\mathbb{E}\phi\left(X_{\tau_{n+1}}\right) \approx \mathbb{E}\phi\left(Y_{\tau_{n+1}}\right)$ for any smooth function ϕ, and so $X_{\tau_{n+1}}$ might be weakly approximated by a random variable z_{n+1} such that the first moments of $z_{n+1} - z_n$ be similar to those of $Y_{\tau_{n+1}} - z_n$. This leads us to the following Local Linearization scheme.

Scheme 1. *Let $\eta_1^1, \ldots, \eta_1^d, \ldots, \eta_N^1, \ldots, \eta_N^d$ be a collection of independent identically distributed symmetric around the mean random variables with zero mean, variance 1 and finite moments of any order. For a given z_0, we define recursively $(z_{n+1})_{n=0,\ldots,N-1}$ by*

$$z_{n+1} = \mu_n(\tau_{n+1}) + \sqrt{\sigma_n(\tau_{n+1}) - \mu_n(\tau_{n+1})\,\mu_n^{\intercal}(\tau_{n+1})}\,\eta_{n+1}, \tag{4}$$

where $\eta_n = \left(\eta_n^1, \ldots, \eta_n^d\right)^{\top}$ and $\mu_n(t)$, $\sigma_n(t)$ satisfy the linear differential equations

$$\mu_n(t) = z_n + \int_{\tau_n}^{t} \left(B_n^0\,\mu_n(s) + b_n^0(s)\right) ds \quad \forall t \in [\tau_n, \tau_{n+1}], \tag{5}$$

$$\sigma_n(t) = z_n z_n^{\top} + \int_{\tau_n}^{t} \mathcal{L}_n(s, \sigma_n(s))\, ds \quad \forall t \in [\tau_n, \tau_{n+1}]. \tag{6}$$

Here

$$\begin{aligned}\mathcal{L}_n(s,\sigma) = {} & \sigma\left(B_n^0\right)^{\top} + B_n^0\,\sigma^{\intercal} + \mu_n(s)\left(b_n^0(s)\right)^{\top} + b_n^0(s)\,\mu_n^{\intercal}(s) \\ & + \sum_{k=1}^{m}\left(B_n^k\,\sigma\left(B_n^k\right)^{\top} + B_n^k\,\mu_n(s)\left(b_n^k(s)\right)^{\top} + b_n^k(s)\,\mu_n^{\intercal}(s)\left(B_n^k\right)^{\top} + b_n^k(s)\left(b_n^k(s)\right)^{\top}\right).\end{aligned} \tag{7}$$

Remark 3.1. From (5) it follows that $\mu_n(\tau_{n+1})$ is the expected valued of $Y_{\tau_{n+1}}$ given $Y_{\tau_n} = z_n$. Moreover, (6) implies

$$\sigma_n(\tau_{n+1}) = \mathbb{E}\left(Y_{\tau_{n+1}} Y_{\tau_{n+1}}^{\top} / Y_{\tau_n} = z_n\right).$$

Remark 3.2. By construction, Scheme 1 preserves the first two moments of the linear equation $dX_t = \sum_{k=0}^{m}(B^k X_t + b^{k,1}t + b^{k,0})dW_t^k$. This includes, for instance, the equations of stochastic oscillators with random frequency and force [13,9], and large systems of stiff linear SDEs that result from the method of lines for linear stochastic partial differential equations [14].

Remark 3.3. By construction, for any stepsize, Scheme 1 preserves the mean-square stability or instability that the solution of the linear equation $dX_t = \sum_{k=0}^{m}(B^k X_t + b^{k,1}t + b^{k,0})dW_t^k$ might have. That is, the stability and instability regions of Scheme 1 match exactly the stability and instability regions of this type of linear equation. For instance, if the trivial solution of the homogeneous equation $dX_t = \sum_{k=0}^{m} B^k X_t dW_t^k$ is mean-square stable [15], Scheme 1 inherits this behavior for any stepsize. That is, if $\lim_{t\to\infty} \mathbb{E}\left(|X_t|^2\right) = 0$, then $\lim_{n\to\infty} \mathbb{E}\left(|Y_n|^2\right) = 0$ for any $\Delta > 0$. Similarly, if X_t is mean-square unstable, them so is Y_n for any stepsize.

Remark 3.4. A key point in the implementation of Scheme 1 is the evaluation of just one matrix exponential for computing $\mu_n(\tau_{n+1})$ and $\sigma_n(\tau_{n+1})$ at each time step. Indeed, from Theorem 2 in [9],

$$\mu_n(\tau_{n+1}) = z_n + L_2 e^{\mathcal{M}_n(\tau_{n+1}-\tau_n)} u_n \tag{8}$$

and

$$vec(\sigma_n(\tau_{n+1})) = L_1 e^{\mathcal{M}_n(\tau_{n+1}-\tau_n)} u_n, \tag{9}$$

where the matrices $\mathcal{M}_n, L_1, L_2$ and the vector u_n are given by

$$\mathcal{M}_n = \begin{bmatrix} \mathcal{A} & \mathcal{B}_5 & \mathcal{B}_4 & \mathcal{B}_3 & \mathcal{B}_2 & \mathcal{B}_1 \\ 0 & \mathcal{C} & I_{d+2} & 0 & 0 & 0 \\ 0 & 0 & \mathcal{C} & 0 & 0 & 0 \\ 0 & 0 & 0 & 0 & 2 & 0 \\ 0 & 0 & 0 & 0 & 0 & 1 \\ 0 & 0 & 0 & 0 & 0 & 0 \end{bmatrix}, \qquad u_n = \begin{bmatrix} vec(z_n z_n^{\intercal}) \\ 0 \\ r \\ 0 \\ 0 \\ 1 \end{bmatrix} \in \mathbb{R}^{d^2+2d+7},$$

$L_2 = \begin{bmatrix} 0_{d\times(d^2+d+2)} & I_d & 0_{d\times 5} \end{bmatrix}$ and $L_1 = \begin{bmatrix} I_{d^2} & 0_{d^2\times(2d+7)} \end{bmatrix}$, with matrices $\mathcal{A}$, $\mathcal{B}_i$, $\mathcal{C}$ and r defined by

$$\mathcal{A} = B_n^0 \oplus B_n^0 + \sum_{k=1}^{m} B_n^k \otimes (B_n^k)^{\intercal}, \qquad \mathcal{C} = \begin{bmatrix} B_n^0 & b_n^{0,1} & B_n^0 z_n + b_n^{0,0} \\ 0 & 0 & 1 \\ 0 & 0 & 0 \end{bmatrix}, \qquad r = \begin{bmatrix} 0_{(d+1)\times 1} \\ 1 \end{bmatrix},$$

$\mathcal{B}_1 = vec(\beta_1) + \beta_4 z_n$, $\mathcal{B}_2 = vec(\beta_2) + \beta_5 z_n$, $\mathcal{B}_3 = vec(\beta_3)$, $\mathcal{B}_4 = \beta_4 L$, and $\mathcal{B}_5 = \beta_5 L$. Here $L = \begin{bmatrix} I_d & 0_{d\times 2} \end{bmatrix}$ and

$$\beta_1 = \sum_{k=1}^{m} b_n^{k,0} (b_n^{k,0})^\intercal, \qquad \beta_2 = \sum_{k=1}^{m} b_n^{k,0} (b_n^{k,1})^\intercal + b_n^{k,1} (b_n^{k,0})^\intercal, \qquad \beta_3 = \sum_{k=1}^{m} b_n^{k,1} (b_n^{k,1})^\intercal,$$

$$\beta_4 = b_n^{0,0} \oplus b_n^{0,0} + \sum_{k=1}^{m} b_n^{k,0} \otimes B_n^k + B_n^k \otimes b_n^{k,0}, \qquad \beta_5 = b_n^{0,1} \oplus b_n^{0,1} + \sum_{k=1}^{m} b_n^{k,1} \otimes B_n^k + B_n^k \otimes b_n^{k,1},$$

being $b_n^{k,0}$ and $b_n^{k,1}$ defined via (2) as $b_n^{k,0} + b_n^{k,1}(s - \tau_n) = b_n^k(s)$. The symbols vec, $\oplus$ and $\otimes$ denote the vectorization operator, the Kronecker sum and the Kronecker product, respectively. I_d is the d-dimensional identity matrix. The matrix exponential in (8) and (9) can be efficiently computed via the Padé method with scaling and squaring strategy or via the Krylov subspace method in the case of large system of SDEs (see, e.g., [16]). For autonomous equations or for equations with additive noise, the matrix exponential in (8) and (9) reduces to simpler forms [9].

Remark 3.5. For SDEs with additive noise, Scheme 1 reduces to the weak order-1 Local Linearization scheme introduced in [8].

Remark 3.6. Scheme 1 is explicit.

4. Rate of convergence

Next theorem establishes the linear rate of weak convergence of Scheme 1 when the drift and diffusion coefficients are smooth enough.

Hypothesis 1. For any $k = 0, \ldots, m$ we have $g^k \in \mathcal{C}_P^4\left([t_0, T] \times \mathbb{R}^d, \mathbb{R}^d\right)$. There exists $C > 0$ such that

$$\left|g^k(t,x)\right| \leq C\left(1 + |x|\right), \qquad \left|\frac{\partial g^k}{\partial t}(t,x)\right| \leq C \quad \text{and} \quad \left|\frac{\partial g^k}{\partial x^j}(t,x)\right| \leq C \tag{10}$$

for all $t \in [t_0, T]$, $x \in \mathbb{R}^d$, $k = 0, \ldots, m$ and $j = 1, \ldots, d$.

Theorem 4.1. *In addition to Hypothesis 1, suppose that X_{t_0} has finite moments of any order and that for all $\phi \in \mathcal{C}_P^4\left(\mathbb{R}^d, \mathbb{R}\right)$,*

$$\left|\mathbb{E}\phi\left(X_{t_0}\right) - \mathbb{E}\phi\left(z_0\right)\right| \leq K\Delta.$$

Then, for all $\phi \in \mathcal{C}_P^4\left(\mathbb{R}^d, \mathbb{R}\right)$,

$$\left|\mathbb{E}\phi\left(X_T\right) - \mathbb{E}\phi\left(z_N\right)\right| \leq K\left(T\right)\Delta,$$

where z_N is given by Scheme 1.

Theorem 4.1 follows from Theorem 14.5.2 of [11] and Lemmata 4.1 and 4.2 given below.

Lemma 4.1. *Under the assumptions of Theorem 4.1, for any $q \geq 1$ we have*

$$\mathbb{E}\left(\max_{n=0,\ldots,N} |z_n|^{2q}\right) \leq K\left(T\right)\left(1 + \mathbb{E}\left(|z_0|^{2q}\right)\right) \tag{11}$$

and

$$\mathbb{E}\left(|z_{n+1} - z_n|^{2q} / \mathfrak{G}_{\tau_n}\right) \leq K\left(T\right)\left(\tau_{k+1} - \tau_k\right)^q \left(1 + |z_n|^{2q}\right) \tag{12}$$

for all $n = 0, \ldots, N-1$, where $\mathfrak{G}_{\tau_n}$ is the σ-sigma algebra generated by X_0, $W_{\tau_n}^k$ and η_n^j with $k = 1, \ldots, m$ and $j = 1, \ldots, d$.

Proof. From (10) we obtain

$$\left|B_n^k\right| \leq d\,C \quad \text{and} \quad \left|b_n^k(s)\right| \leq C\left(1 + |z_n|\right) + d\,C\,|z_n| + C\left(s - \tau_n\right) \tag{13}$$

for all $n = 0, \ldots, N-1$, $k = 0, \ldots, m$ and $s \in [\tau_n, \tau_{n+1}]$. Here and subsequently, the norm $|\cdot|$ on $\mathbb{R}^{d\times d}$ is the operator norm induced by the Euclidean norm of vectors, which is indeed the spectral matrix norm. Then, combining Gronwall's lemma with (5) gives

$$|\mu_n(s)| \leq \exp\Big(d\,C\left(s - \tau_n\right)\Big)\left(\left(1 + (d+1)\,C\Delta\right)|z_n| + C\Delta + C\Delta^2/2\right) \quad \forall s \in [\tau_n, \tau_{n+1}]. \tag{14}$$

Since $\left|x y^{\top}\right| = |x|\,|y|$ for any $x, y \in \mathbb{R}^d$,

$$|\mathcal{L}_n(s,\sigma)| \leq \left(2d\,C + md^2C^2\right)|\sigma| + 2\,|\mu_n(s)|\left|b_n^0(s)\right| + \sum_{k=1}^{m}\left(2d\,C\,|\mu_n(s)|\left|b_n^k(s)\right| + \left|b_n^k(s)\right|^2\right),$$

where $\mathcal{L}_n$ is defined in (7). Therefore, (13) and (14) lead to

$$|\mathcal{L}_n(s,\sigma)| \leq \left(2d\,C + md^2C^2\right)|\sigma| + K(T)\left(1+|z_n|^2\right) \quad \forall s \in [\tau_n, \tau_{n+1}], \tag{15}$$

for all $n = 0, \ldots, N-1$. Using Gronwall's lemma, (6) and (15) we deduce that

$$|\sigma_n(s)| \leq K(T)\left(1+|z_n|^2\right) \quad \forall s \in [\tau_n, \tau_{n+1}]. \tag{16}$$

Decomposing

$$\widetilde{\sigma}_n(t) := \sigma_n(t) - \mu_n(t)\,\mu_n^{\top}(t)$$

as $\sigma_n(t) - z_n z_n^{\top} - z_n(\mu_n(t) - z_n)^{\top} - (\mu_n(t) - z_n)\,z_n^{\top} - (\mu_n(t) - z_n)(\mu_n(t) - z_n)^{\top}$ we have

$$\begin{aligned}\widetilde{\sigma}_n(t) = {} & \int_{\tau_n}^{t}\mathcal{L}_n(s,\sigma_n(s))\,ds - z_n\left(\int_{\tau_n}^{t}\left(B_n^0\,\mu_n(s) + b_n^0(s)\right)ds\right)^{\top} - \int_{\tau_n}^{t}\left(B_n^0\,\mu_n(s) + b_n^0(s)\right)ds\,z_n^{\top} \\ & - \int_{\tau_n}^{t}\left(B_n^0\,\mu_n(s) + b_n^0(s)\right)ds\left(\int_{\tau_n}^{t}\left(B_n^0\,\mu_n(s) + b_n^0(s)\right)ds\right)^{\top},\end{aligned}$$

and so (14)–(16) yields

$$|\widetilde{\sigma}_n(t)| \leq K(T)\left(1+|z_n|^2\right)(t-\tau_n) \quad \forall t \in [\tau_n, \tau_{n+1}]. \tag{17}$$

Since $\widetilde{\sigma}_k(\tau_{k+1})$ is a positive semi-definite matrix and $|\cdot|$ is the spectral matrix norm, $\left|\sqrt{\widetilde{\sigma}_k(\tau_{k+1})}\right|^2 = |\widetilde{\sigma}_k(\tau_{k+1})|$. We thus get

$$\begin{aligned}\left|\sqrt{\widetilde{\sigma}_n(\tau_{n+1})}\,\eta_{n+1}\right|^{2q} &\leq |\widetilde{\sigma}_n(\tau_{n+1})|^q\,|\eta_{n+1}|^{2q} \\ &\leq K(T)\left(1+|z_n|^{2q}\right)(\tau_{n+1}-\tau_n)^q\,|\eta_{n+1}|^{2q}.\end{aligned} \tag{18}$$

Substituting (5) into (4) and replacing n by k we have

$$z_{k+1} = z_k + \int_{\tau_k}^{\tau_{k+1}}\left(B_k^0\,\mu_k(s) + b_k^0(s)\right)ds + \sqrt{\sigma_k(\tau_{k+1}) - \mu_k(\tau_{k+1})\,\mu_k^{\intercal}(\tau_{k+1})}\,\eta_{k+1}.$$

Evaluating this recursive expression from $k = 0$ until $k = n$ we obtain

$$z_{n+1} = z_0 + \int_{t_0}^{\tau_{n+1}}\left(B_{n(s)}^0\,\mu_{n(s)}(s) + b_{n(s)}^0(s)\right)ds + S_{n+1}, \tag{19}$$

where $n(t) = \max\{n = 0, \ldots, N : \tau_n \leq t\}$ and

$$S_{n+1} = \sum_{k=0}^{n}\sqrt{\sigma_k(\tau_{k+1}) - \mu_k(\tau_{k+1})\,\mu_k^{\intercal}(\tau_{k+1})}\,\eta_{k+1}.$$

Applying Hölder's inequality for integrals we deduce that for all $q \geq 1$,

$$\begin{aligned}\left|\int_{t_0}^{\tau_{n+1}}\left(B_{n(s)}^0\,\mu_{n(s)}(s) + b_{n(s)}^0(s)\right)ds\right| &\leq (\tau_{n+1}-t_0)^{\frac{2q-1}{2q}}\left(\int_{t_0}^{\tau_{n+1}}\left|\left(B_{n(s)}^0\,\mu_{n(s)}(s) + b_{n(s)}^0(s)\right)\right|^{2q}ds\right)^{1/2q} \\ &\leq T^{\frac{2q-1}{2q}}\left(\int_{t_0}^{\tau_{n+1}}\left(d\,C\left|\mu_{n(s)}(s)\right| + \left|b_{n(s)}^0(s)\right|\right)^{2q}ds\right)^{1/2q}.\end{aligned}$$

Hence, (13) and (14) yield

$$\begin{aligned}\left|\int_{t_0}^{\tau_{n+1}}\left(B_{n(s)}^0\,\mu_{n(s)}(s) + b_{n(s)}^0(s)\right)ds\right|^{2q} &\leq K(T)\left(1 + \int_{t_0}^{\tau_{n+1}}\left|z_{n(s)}\right|^{2q}ds\right) \\ &\leq K(T)\left(1 + \sum_{k=0}^{n}(\tau_{k+1}-\tau_k)\,|z_k|^{2q}\right).\end{aligned} \tag{20}$$

Since the random variable η_k^ℓ is symmetric around its zero mean, all its odd moments are zero. Using this, we obtain that

$$\begin{aligned}\mathbb{E}\left(|S_{n+1}|^2\right) &= \mathbb{E}(S_{n+1}^\intercal S_{n+1}) \\ &= \sum_{k=0}^{n} \mathbb{E}\left(\eta_{k+1}^\intercal \left(\sigma_k(\tau_{k+1}) - \mu_k(\tau_{k+1})\,\mu_k^\intercal(\tau_{k+1})\right)\eta_{k+1}\right) \\ &= \sum_{k=0}^{n}\sum_{\ell=1}^{d} \mathbb{E}\left(\sigma_k^{\ell,\ell}(\tau_{k+1}) + \left(\mu_k^\ell(\tau_{k+1})\right)^2\right)\end{aligned}$$

for all $n = 0, \ldots, N-1$, where $S_0 = 0$ and the superscripts ℓ and ℓ, ℓ denote, respectively, the elements of vectors and the diagonal entries of matrices. In addition, since $\sigma_k(\tau_{k+1}) = \mathbb{E}\left(Y_{\tau_{k+1}} Y_{\tau_{k+1}}^\top / \mathfrak{G}_{\tau_k}\right)$, (14) yields

$$\mathbb{E}\left(|S_{n+1}|^2\right) \le \sum_{k=0}^{n}\left(\mathbb{E}\left(\left|Y_{\tau_{k+1}}\right|^2\right) + \mathbb{E}\left|\mu_k(\tau_{k+1})\right|^2\right) < +\infty,$$

and so $(S_n)_{n=0,\ldots,N}$ is a $\left(\mathfrak{G}_{\tau_n}\right)_{n=0,\ldots,N}$-square integrable martingale. According to the Burkholder–Davis–Gundy inequality (see, e.g., [17]) we have

$$\mathbb{E}\left(\max_{k=0,\ldots,n}\left(S_{k+1}^\ell\right)^{2q}\right) \le C_q \mathbb{E}\left(\sum_{k=0}^{n}\left(\left(\sqrt{\widetilde{\sigma}_k(\tau_{k+1})}\,\eta_{k+1}\right)^\ell\right)^2\right)^q, \tag{21}$$

where C_q is a positive constant, and the superscript ℓ stands for the ℓth coordinate of vectors.

From the Hölder inequality for series it is obtained that

$$\left(\sum_{i=0}^{\ell} a_i\right)^\kappa \le \ell^{\kappa-1}\sum_{i=0}^{\ell} a_i^\kappa \tag{22}$$

for all $\kappa, \ell \in \mathbb{N}_+$ and $a_i \ge 0$.

Combining (22) with (21) we have

$$\begin{aligned}\mathbb{E}\left(\max_{k=0,\ldots,n}|S_{k+1}|^{2q}\right) &\le d^{q-1}\sum_{\ell=1}^{d}\mathbb{E}\left(\max_{k=0,\ldots,n}\left(S_{k+1}^\ell\right)^{2q}\right) \\ &\le d^{q-1}C_q\sum_{\ell=1}^{d}\mathbb{E}\left(\sum_{k=0}^{n}\left(\left(\sqrt{\widetilde{\sigma}_k(\tau_{k+1})}\,\eta_{k+1}\right)^\ell\right)^2\right)^q,\end{aligned}$$

and applying Hölder's inequality for series gives

$$\begin{aligned}\left(\sum_{k=0}^{n}\left(\left(\sqrt{\widetilde{\sigma}_k(\tau_{k+1})}\,\eta_{k+1}\right)^\ell\right)^2\right)^q &= \left(\sum_{k=0}^{n}(\tau_{k+1}-\tau_k)^{1/p}(\tau_{k+1}-\tau_k)^{1/q}\left(\left(\sqrt{\widetilde{\sigma}_k(\tau_{k+1})}\,\eta_{k+1}\right)^\ell\right)^2/(\tau_{k+1}-\tau_k)\right)^q \\ &\le \left(\sum_{k=0}^{n}(\tau_{k+1}-\tau_k)\right)^{q-1}\sum_{k=0}^{n}(\tau_{k+1}-\tau_k)\left(\left(\sqrt{\widetilde{\sigma}_k(\tau_{k+1})}\,\eta_{k+1}\right)^\ell\right)^{2q}/(\tau_{k+1}-\tau_k)^q\end{aligned}$$

with $1/p + 1/q = 1$. From the last two inequalities, (18) and the independent identically distributed condition of the set of random variables η_{k+1}^ℓ we obtain that

$$\begin{aligned}\mathbb{E}\left(\max_{k=0,\ldots,n}|S_{k+1}|^{2q}\right) &\le (Td)^{q-1}C_q\mathbb{E}\left(\sum_{k=0}^{n}(\tau_{k+1}-\tau_k)\left(\sum_{\ell=1}^{d}\left(\left(\sqrt{\widetilde{\sigma}_k(\tau_{k+1})}\,\eta_{k+1}\right)^\ell\right)^2\right)^q/(\tau_{k+1}-\tau_k)^q\right) \\ &= (Td)^{q-1}C_q\sum_{k=0}^{n}\mathbb{E}\left((\tau_{k+1}-\tau_k)\left|\sqrt{\widetilde{\sigma}_k(\tau_{k+1})}\,\eta_{k+1}\right|^{2q}/(\tau_{k+1}-\tau_k)^q\right) \\ &\le K(T)\,\mathbb{E}\left(|\eta_1|^{2q}\right)\left(T + \sum_{k=0}^{n}(\tau_{k+1}-\tau_k)\,\mathbb{E}(|z_k|^{2q})\right).\end{aligned} \tag{23}$$

On the other hand, using (19) and (22) yields

$$|z_{n+1}|^{2q} \le 3^{2q-1}\left(|z_0|^{2q} + \left|\int_{t_0}^{\tau_{n+1}}\left(B_{n(s)}^0\,\mu_{n(s)}(s) + b_{n(s)}^0(s)\right)ds\right|^{2q} + |S_{n+1}|^{2q}\right).$$

This, (20) and (23) imply that

$$\mathbb{E}\left(\max_{j=0,\ldots,n+1}\left|z_j\right|^{2q}\right) \leq K\left(T\right)\left(\mathbb{E}\left|z_0\right|^{2q}+1+\sum_{k=0}^{n}\left(\tau_{k+1}-\tau_k\right)\mathbb{E}(|z_k|^{2q})\right).$$

The discrete time Gronwall–Bellman lemma now leads to (11).

We proceed to show (12). Using Hölder's inequality for integrals, (13) and (14) we obtain

$$\begin{aligned}\left|\int_{\tau_n}^{\tau_{n+1}}\left(B_n^0\,\mu_n\left(s\right)+b_n^0\left(s\right)\right)ds\right|^{2q} &\leq \left(\tau_{n+1}-\tau_n\right)^{2q-1}\int_{\tau_n}^{\tau_{n+1}}\left(\left|B_n^0\right|\left|\mu_n\left(s\right)\right|+\left|b_n^0\left(s\right)\right|\right)^{2q}ds\\ &\leq K\left(T\right)\left(\tau_{n+1}-\tau_n\right)^{2q}\left(1+\left|z_n\right|^{2q}\right),\end{aligned} \tag{24}$$

and from (18) we have

$$\mathbb{E}\left(\left|\sqrt{\widetilde{\sigma}_n\left(\tau_{n+1}\right)}\,\eta_{n+1}\right|^{2q}/\mathfrak{G}_{\tau_n}\right) \leq K\left(T\right)\left(1+\left|z_n\right|^{2q}\right)\left(\tau_{n+1}-\tau_n\right)^{q}\mathbb{E}\left(\left|\eta_{n+1}\right|^{2q}/\mathfrak{G}_{\tau_n}\right). \tag{25}$$

Applying (4) and the algebraic inequality (22) we obtain

$$\begin{aligned}\mathbb{E}\left(\left|z_{n+1}-z_n\right|^{2q}/\mathfrak{G}_{\tau_n}\right) \leq\ & 2^{2q-1}\mathbb{E}\left(\left|\int_{\tau_n}^{\tau_{n+1}}\left(B_n^0\,\mu_n\left(s\right)+b_n^0\left(s\right)\right)ds\right|^{2q}/\mathfrak{G}_{\tau_n}\right)\\ &+2^{2q-1}\mathbb{E}\left(\left|\sqrt{\widetilde{\sigma}_n\left(\tau_{n+1}\right)}\,\eta_{n+1}\right|^{2q}/\mathfrak{G}_{\tau_n}\right).\end{aligned}$$

This, together with (24) and (25), implies (12). □

Lemma 4.2. *Assume the hypothesis of Theorem 4.1. Let*

$$\chi_{n+1}=f\left(\tau_n,z_n\right)\left(\tau_{n+1}-\tau_n\right)+\sum_{k=1}^{m}g^k\left(\tau_n,z_n\right)\left(W_{\tau_{n+1}}^k-W_{\tau_n}^k\right). \tag{26}$$

Then, for all $n=0,\ldots,N-1$,

$$\left|\mathbb{E}\left(\left(z_{n+1}-z_n\right)/\mathfrak{G}_{\tau_n}\right)-\mathbb{E}\left(\chi_{n+1}/\mathfrak{G}_{\tau_n}\right)\right| \leq K\left(T\right)\left(\tau_{n+1}-\tau_n\right)^2\left(1+\left|z_n\right|\right), \tag{27}$$

$$\left|\mathbb{E}\left(\left(z_{n+1}-z_n\right)\left(z_{n+1}-z_n\right)^{\top}/\mathfrak{G}_{\tau_n}\right)-\mathbb{E}\left(\chi_{n+1}\chi_{n+1}^{\top}/\mathfrak{G}_{\tau_n}\right)\right| \leq K\left(T\right)\left(\tau_{n+1}-\tau_n\right)^2\left(1+\left|z_n\right|^2\right) \tag{28}$$

and

$$\begin{aligned}&\left|\mathbb{E}\left(\left(z_{n+1}-z_n\right)^{\ell}\left(z_{n+1}-z_n\right)\left(z_{n+1}-z_n\right)^{\top}/\mathfrak{G}_{\tau_n}\right)-\mathbb{E}\left(\chi_{n+1}^{\ell}\chi_{n+1}\chi_{n+1}^{\top}/\mathfrak{G}_{\tau_n}\right)\right|\\ &\quad\leq K\left(T\right)\left(\tau_{n+1}-\tau_n\right)^2\left(1+\left|z_n\right|^2\right),\end{aligned} \tag{29}$$

where the superscript ℓ *denotes the* ℓ*th element of vectors, and* $\mathfrak{G}_{\tau_n}$ *is the* σ*-sigma algebra generated by* X_0, $W_{\tau_n}^k$ *and* η_n^j *with* $k=1,\ldots,m$ *and* $j=1,\ldots,d$.

Proof. From (2) it follows that $f\left(\tau_n,z_n\right)=B_n^0\,z_n+b_n^0\left(\tau_n\right)$, and so (5) implies

$$\begin{aligned}\mu_n\left(\tau_{n+1}\right)-z_n-f\left(\tau_n,z_n\right)\left(\tau_{n+1}-\tau_n\right) &= \int_{\tau_n}^{\tau_{n+1}}\left(B_n^0\,\mu_n\left(s\right)+b_n^0\left(s\right)-f\left(\tau_n,z_n\right)\right)ds\\ &= \int_{\tau_n}^{\tau_{n+1}}\left(B_n^0\left(\mu_n\left(s\right)-z_n\right)+b_n^0\left(s\right)-b_n^0\left(\tau_n\right)\right)ds.\end{aligned}$$

Applying (10) gives

$$\begin{aligned}\left|\mu_n\left(\tau_{n+1}\right)-z_n-f\left(\tau_n,z_n\right)\left(\tau_{n+1}-\tau_n\right)\right| &\leq \int_{\tau_n}^{\tau_{n+1}}\left(d\,C\left|\mu_n\left(s\right)-z_n\right|+C\left(s-\tau_n\right)\right)ds\\ &\leq d\,C\int_{\tau_n}^{\tau_{n+1}}\int_{\tau_n}^{s}\left|B_n^0\,\mu_n\left(r\right)+b_n^0\left(r\right)\right|drds+C^2\left(\tau_{n+1}-\tau_n\right)^2/2.\end{aligned}$$

Therefore, using (13) and (14) we deduce that

$$\left|\mu_n\left(\tau_{n+1}\right)-z_n-f\left(\tau_n,z_n\right)\left(\tau_{n+1}-\tau_n\right)\right| \leq K\left(T\right)\left(\tau_{n+1}-\tau_n\right)^2\left(1+\left|z_n\right|\right). \tag{30}$$

Due to the symmetry of the random variables η_{n+1}^{ℓ} and $W_{\tau_{n+1}}^{k} - W_{\tau_n}^{k}$,

$$\left|\mathbb{E}\left(\left(z_{n+1}-z_n\right)/\mathfrak{G}_{\tau_n}\right) - \mathbb{E}\left(\chi_{n+1}/\mathfrak{G}_{\tau_n}\right)\right| = \left|\mu_n\left(\tau_{n+1}\right) - z_n - f\left(\tau_n, z_n\right)\left(\tau_{n+1}-\tau_n\right)\right|,$$

and so (30) yields (27).

By the definition (26) of χ_{n+1},

$$\mathbb{E}\left(\chi_{n+1}\chi_{n+1}^{\top}/\mathfrak{G}_{\tau_n}\right) = f\left(\tau_n, z_n\right) f^{\top}\left(\tau_n, z_n\right)\left(\tau_{n+1}-\tau_n\right)^2 + \sum_{k=1}^{m} g^k\left(\tau_n, z_n\right)\left(g^k\left(\tau_n, z_n\right)\right)^{\top}\left(\tau_{n+1}-\tau_n\right),$$

and hence (10) leads to

$$\left|\mathbb{E}\left(\chi_{n+1}\chi_{n+1}^{\top}/\mathfrak{G}_{\tau_n}\right) - \sum_{k=1}^{m} g^k\left(\tau_n, z_n\right)\left(g^k\left(\tau_n, z_n\right)\right)^{\top}\left(\tau_{n+1}-\tau_n\right)\right| \leq 2C^2\left(\tau_{n+1}-\tau_n\right)^2\left(1+|z_n|^2\right). \tag{31}$$

From (4), we get

$$\mathbb{E}\left(\left(z_{n+1}-z_n\right)\left(z_{n+1}-z_n\right)^{\top}/\mathfrak{G}_{\tau_n}\right) = \left(\mu_n\left(\tau_{n+1}\right)-z_n\right)\left(\mu_n\left(\tau_{n+1}\right)-z_n\right)^{\top} + \widetilde{\sigma}_n\left(\tau_{n+1}\right),$$

where $\widetilde{\sigma}_n(t) = \sigma_n(t) - \mu_n(t)\,\mu_n^{\intercal}(t)$ for any $t \in [\tau_n, \tau_{n+1}]$. Since

$$\begin{aligned}\widetilde{\sigma}_n\left(\tau_{n+1}\right) = {} & \sigma_n\left(\tau_{n+1}\right) - z_n z_n^{\top} - z_n\left(\mu_n\left(\tau_{n+1}\right)-z_n\right)^{\top} - \left(\mu_n\left(\tau_{n+1}\right)-z_n\right) z_n^{\top} \\ & - \left(\mu_n\left(\tau_{n+1}\right)-z_n\right)\left(\mu_n\left(\tau_{n+1}\right)-z_n\right)^{\top},\end{aligned}$$

inequality (30) yields

$$\begin{aligned}R_1 &:= \left|\mathbb{E}\left(\left(z_{n+1}-z_n\right)\left(z_{n+1}-z_n\right)^{\top}/\mathfrak{G}_{\tau_n}\right) - \sigma_n\left(\tau_{n+1}\right) + z_n z_n^{\top} + \left(z_n f^{\top}\left(\tau_n, z_n\right) + f\left(\tau_n, z_n\right) z_n^{\top}\right)\left(\tau_{n+1}-\tau_n\right)\right| \\ &\leq K(T)\left(\tau_{n+1}-\tau_n\right)^2\left(1+|z_n|^2\right).\end{aligned}$$

Using (13)–(15), together with Hypothesis 1, we deduce that

$$\left|\mathcal{L}_n\left(s, \sigma_n(s)\right) - \mathcal{L}_n\left(\tau_n, z_n z_n^{\top}\right)\right| \leq K(T)\left(s-\tau_n\right)\left(1+|z_n|^2\right),$$

and so

$$\begin{aligned}R_2 &:= \left|\sigma_n\left(\tau_{n+1}\right) - z_n z_n^{\top} - \mathcal{L}_n\left(\tau_n, z_n z_n^{\top}\right)\left(\tau_{n+1}-\tau_n\right)\right| \\ &\leq \int_{\tau_n}^{\tau_{n+1}} \left|\mathcal{L}_n\left(s, \sigma_n(s)\right) - \mathcal{L}_n\left(\tau_n, z_n z_n^{\top}\right)\right| ds \\ &\leq K(T)\left(\tau_{n+1}-\tau_n\right)^2\left(1+|z_n|^2\right).\end{aligned}$$

By taking into account that

$$\mathcal{L}_n\left(\tau_n, z_n z_n^{\top}\right) = z_n f^{\top}\left(\tau_n, z_n\right) + f\left(\tau_n, z_n\right) z_n^{\top} + \sum_{k=1}^{m} g^k\left(\tau_n, z_n\right)\left(g^k\left(\tau_n, z_n\right)\right)^{\top},$$

we have

$$\begin{aligned}&\left|\mathbb{E}\left(\left(z_{n+1}-z_n\right)\left(z_{n+1}-z_n\right)^{\top}/\mathfrak{G}_{\tau_n}\right) - \sum_{k=1}^{m} g^k\left(\tau_n, z_n\right)\left(g^k\left(\tau_n, z_n\right)\right)^{\top}\left(\tau_{n+1}-\tau_n\right)\right| \\ &= \left|\mathbb{E}\left(\left(z_{n+1}-z_n\right)\left(z_{n+1}-z_n\right)^{\top}/\mathfrak{G}_{\tau_n}\right) - \left(\mathcal{L}_n\left(\tau_n, z_n z_n^{\top}\right) - z_n f^{\top}\left(\tau_n, z_n\right) - f\left(\tau_n, z_n\right) z_n^{\top}\right)\left(\tau_{n+1}-\tau_n\right)\right| \\ &\leq R_1 + R_2.\end{aligned} \tag{32}$$

We now combine (31) with (32) to obtain (28).

From the symmetry of the random variable $W_{\tau_{n+1}}^{k} - W_{\tau_n}^{k}$, a careful computation shows

$$\begin{aligned}\mathbb{E}\left(\chi_{n+1}^{\ell}\chi_{n+1}\chi_{n+1}^{\top}/\mathfrak{G}_{\tau_n}\right) = {} & f^{\ell}\left(\tau_n, z_n\right) f\left(\tau_n, z_n\right) f^{\top}\left(\tau_n, z_n\right)\left(\tau_{n+1}-\tau_n\right)^3 + f^{\ell}\left(\tau_n, z_n\right) G_n G_n^{\top}\left(\tau_{n+1}-\tau_n\right)^2 \\ & + f\left(\tau_n, z_n\right)\left(G_n G_n^{\top}\right)^{\ell,\cdot}\left(\tau_{n+1}-\tau_n\right)^2 + \left(G_n G_n^{\top}\right)^{\cdot,\ell} f^{\top}\left(\tau_n, z_n\right)\left(\tau_{n+1}-\tau_n\right)^2,\end{aligned}$$

where G_n is the $\mathbb{R}^{d\times m}$-matrix whose (i,j)th entry is the ith element of $g^j(\tau_n, z_n)$. Similarly, using the symmetry of the random variable η_{n+1}^{ℓ}, we obtain

$$\begin{aligned}&\mathbb{E}\left(\left(z_{n+1}-z_n\right)^{\ell}\left(z_{n+1}-z_n\right)\left(z_{n+1}-z_n\right)^{\top}/\mathfrak{G}_{\tau_n}\right) \\ &= \left(\mu_n\left(\tau_{n+1}\right)-z_n\right)^{\ell}\widetilde{\sigma}_n\left(\tau_{n+1}\right) + \left(\mu_n\left(\tau_{n+1}\right)-z_n\right)\widetilde{\sigma}_n^{\ell,\cdot}\left(\tau_{n+1}\right) \\ &\quad + \widetilde{\sigma}_n^{\cdot,\ell}\left(\tau_{n+1}\right)\left(\mu_n\left(\tau_{n+1}\right)-z_n\right)^{\top} + \left(\mu_n\left(\tau_{n+1}\right)-z_n\right)^{\ell}\left(\mu_n\left(\tau_{n+1}\right)-z_n\right)\left(\mu_n\left(\tau_{n+1}\right)-z_n\right)^{\top}.\end{aligned}$$

Inequality (29) results from the last two expressions together with (10), (17) and

$$|\mu_n(\tau_{n+1}) - z_n| \leq \int_{\tau_n}^{\tau_{n+1}} \left| B_n^0 \mu_n(s) + b_n^0(s) \right| ds \leq K(T)(\tau_{n+1} - \tau_n)(1 + |z_n|).$$

This completes the proof. □

Remark 4.1. Theorem 4.1 states that Scheme 1 converges weakly to the solution of the SDE (1) with order 1. However, this order of convergence might be higher for certain particular classes of equations. For instance, when the diffusion coefficient $g^k \equiv 0$, for $k = 1, \ldots, m$, Scheme 1 reduces to the classical Local Linearization method for ordinary differential equations (ODEs) [18]. This deterministic method has order 2 of convergence for nonlinear ODEs but, depending on its numerical implementation, it has usually higher order for linear ODEs [6]. It is known that, for SDEs with small noise, integrators with "deterministic" high order (but low stochastic order) often yield far smaller errors with larger step size than schemes with "deterministically" same order as in the stochastic sense (see, e.g., [19]). From this perspective, Scheme 1 has other clear advantage.

5. Numerical simulations

In this section, numerical simulations are presented in order to illustrate the performance of Scheme 1. This involves the numerical calculation of known expressions for functionals of two SDEs: a bilinear equation with random oscillatory dynamics, and a renowned nonlinear test equation. The Padé method with scaling and squaring strategy (see, e.g., [16]) was used to compute the matrix exponential in (8) and (9), whereas the square root of the matrix $\sigma_n(\tau_{n+1}) - \mu_n(\tau_{n+1})\,\mu_n^{\intercal}(\tau_{n+1})$ in (4) was computed by means of the singular value decomposition (see, e.g., [20]). η_n^k in (4) was set as a two-point distributed random variable with probability $P(\eta_n^k = \pm 1) = 1/2$ for all $n = 1, \ldots, N$ and $k = 1, \ldots, m$.

In addition, the simulation results of Scheme 1 are compared with those of the Trapezoidal and Balanced methods considered in [21,22], which have the same mean square stability of the new method (see, e.g., [22,21,15]). We recall that, on a uniform time partition $\tau_n = n\Delta$ with $\Delta > 0$ and $n = 0, 1, \ldots$, these Trapezoidal and Balanced methods for the SDE (1) are respectively defined by the recursive expressions

$$z_{n+1} = z_n + (1-\theta) f(\tau_n, z_n)\Delta + \theta f(\tau_{n+1}, z_{n+1})\Delta + \sum_{k=1}^{m} g^k(\tau_n, z_n)(W^k_{\tau_{n+1}} - W^k_{\tau_n}) \tag{33}$$

with $\theta = 0.5$, and

$$\begin{aligned} z_{n+1} = {} & z_n + f(\tau_n, z_n)\Delta + \sum_{k=1}^{m} g^k(\tau_n, z_n)(W^k_{\tau_{n+1}} - W^k_{\tau_n}) \\ & + c^0(\tau_n, z_n)\Delta(z_n - z_{n+1}) + \sum_{k=1}^{m} c^k(\tau_n, z_n)\left| W^k_{\tau_{n+1}} - W^k_{\tau_n} \right| (z_n - z_{n+1}) \end{aligned}$$

with $c^0(\tau_n, z_n) = -0.5B_n^0$, $c^k(\tau_n, z_n) = \sqrt{(B_n^k)^{\intercal} B_n^k}$ for $k = 1, \ldots, m$, and B_n^k defined as at the beginning of Section 3. As difference with Scheme 1, these two methods are semi-implicit and implicit, respectively, and their first two conditional moments do not match those of $dX_t = \sum_{k=0}^{m}(B^k X_t + b^{k,1} t + b^{k,0})dW_t^k$. Eventually, some comparison with the Euler–Romberg extrapolation method introduced in [23] and the Euler method is also presented. With the Euler–Romberg extrapolation method the expected value $\mathbb{E}\phi\left(X_{t_{n+1}}\right)$ is approximated by $2\mathbb{E}\phi\left(z_{n+1}^{\Delta/2}\right) - \mathbb{E}\phi\left(z_{n+1}\right)$ for all $n = 0, 1, \ldots$ and smooth functional ϕ, where z_{n+1} is the Euler method with stepsize Δ defined by (33) with $\theta = 0$, and $z_{n+1}^{\Delta/2}$ is also the Euler method but with stepsize $\Delta/2$. For the mentioned methods, $z_0 = X_0$, where X_0 is the initial condition of the SDE (1) at $t_0 = 0$.

A Matlab code was elaborated for each one of these integrators and all the simulations were carried out in Matlab2014a.

Example 1 (*Bilinear SDE with Random Oscillatory Dynamics*)**.**

$$dX_t = \alpha \begin{bmatrix} 0 & 1 \\ -1 & 0 \end{bmatrix} X_t dt + \rho_1 \begin{bmatrix} 0 & 1 \\ -1 & 0 \end{bmatrix} X_t dW_t^1 + \rho_2 \begin{bmatrix} 1 & 0 \\ 0 & 1 \end{bmatrix} X_t dW_t^2, \tag{34}$$

for all $t \in [0, 12.5625]$, initial condition $(X_0^1, X_0^2) = (1, 2)$, and parameters $\alpha = 10$, $\rho_1 = 0.1$ and $\rho_2 = 2\rho_1$.

Since $\begin{bmatrix} 1 & 0 \\ 0 & 1 \end{bmatrix}$ commutes with $\begin{bmatrix} 0 & 1 \\ -1 & 0 \end{bmatrix}$, the solution of (34) is given by

$$X_t = \exp\left(\begin{bmatrix} (\rho_1^2 - \rho_2^2)/2 & \alpha \\ -\alpha & (\rho_1^2 - \rho_2^2)/2 \end{bmatrix} t + \begin{bmatrix} 0 & \rho_1 \\ -\rho_1 & 0 \end{bmatrix} W_t^1 + \begin{bmatrix} \rho_2 & 0 \\ 0 & \rho_2 \end{bmatrix} W_t^2 \right) \tag{35}$$

(see, e.g., [24], p. 144). From Theorem 3 in [9], the mean m_t and variance v_t of X_t are given by the expressions

$$m_t = X_0 + L_2 \exp(Ht) u_0 \tag{36}$$

and

$$vec(v_t) = L_1 \exp(Ht) u_0 - vec(m_t m_t^\intercal), \tag{37}$$

where the matrices L_1, L_2, H and the vector u_0 are defined as

$$H = \begin{bmatrix} A & 0 & 0 \\ 0 & 0 & 0 \\ 0 & 0 & C \end{bmatrix} \in \mathbb{R}^{8\times 8}, \qquad u_0 = \begin{bmatrix} vec(X_0 X_0^\intercal) \\ 1 \\ r \end{bmatrix} \in \mathbb{R}^8,$$

$$L_1 = [I_4 \quad 0_4] \in \mathbb{R}^{4\times 8} \quad \text{and} \quad L_2 = [0_{2\times 5} \quad I_2 \quad 0_{2\times 1}] \in \mathbb{R}^{2\times 8}$$

with

$$A = \begin{bmatrix} \rho_2^2 & \alpha & \alpha & \rho_1^2 \\ -\alpha & \rho_2^2 & -\rho_1^2 & \alpha \\ -\alpha & -\rho_1^2 & \rho_2^2 & \alpha \\ \rho_1^2 & -\alpha & -\alpha & \rho_2^2 \end{bmatrix} \in \mathbb{R}^{4\times 4}, \qquad C = \begin{bmatrix} 0 & \alpha & \alpha X_0^2 \\ -\alpha & 0 & -\alpha X_0^1 \\ 0 & 0 & 0 \end{bmatrix} \in \mathbb{R}^{3\times 3} \quad \text{and} \quad r = \begin{bmatrix} 0 \\ 0 \\ 1 \end{bmatrix} \in \mathbb{R}^3.$$

First, we compare the exact values (36)–(37) for the mean and variance of X_t with their estimates obtained via Monte Carlo simulations. For this purpose, M realizations $X_{\tau_n}^{\{i\}}$ of the exact solution and $z_n^{\{i\}}$ of Scheme 1 were computed on a uniform time partition $\tau_n = n\Delta$, with $\Delta = 1/2^6$, $n = 0, \ldots, N$, and $N = 804$. Then, with the estimates

$$\overline{m}_{\tau_n} = \frac{1}{M}\sum_{i=1}^{M} X_{\tau_n}^{\{i\}} \quad \text{and} \quad \widehat{m}_{\tau_n} = \frac{1}{M}\sum_{i=1}^{M} z_n^{\{i\}}$$

for the mean, and

$$\overline{v}_{\tau_n} = \frac{1}{M}\sum_{i=1}^{M} X_{\tau_n}^{\{i\}} (X_{\tau_n}^{\{i\}})^\intercal - \overline{m}_{\tau_n}\overline{m}_{\tau_n}^\intercal \quad \text{and} \quad \widehat{v}_{\tau_n} = \frac{1}{M}\sum_{i=1}^{M} z_n^{\{i\}} (z_n^{\{i\}})^\intercal - \widehat{m}_{\tau_n}\widehat{m}_{\tau_n}^\intercal$$

for the variance, the errors

$$\begin{aligned}
\overline{e}_{\tau_n}^{[1]} &= \left|m_{\tau_n}^1 - \overline{m}_{\tau_n}^1\right| \quad \text{and} \quad \widehat{e}_{\tau_n}^{[1]} = \left|m_{\tau_n}^1 - \widehat{m}_{\tau_n}^1\right| \\
\overline{e}_{\tau_n}^{[2]} &= \left|m_{\tau_n}^2 - \overline{m}_{\tau_n}^2\right| \quad \text{and} \quad \widehat{e}_{\tau_n}^{[2]} = \left|m_{\tau_n}^2 - \widehat{m}_{\tau_n}^2\right| \\
\overline{e}_{\tau_n}^{[3]} &= \left|v_{\tau_n}^{1,1} - \overline{v}_{\tau_n}^{1,1}\right| \quad \text{and} \quad \widehat{e}_{\tau_n}^{[3]} = \left|v_{\tau_n}^{1,1} - \widehat{v}_{\tau_n}^{1,1}\right| \\
\overline{e}_{\tau_n}^{[4]} &= \left|v_{\tau_n}^{2,2} - \overline{v}_{\tau_n}^{2,2}\right| \quad \text{and} \quad \widehat{e}_{\tau_n}^{[4]} = \left|v_{\tau_n}^{2,2} - \widehat{v}_{\tau_n}^{2,2}\right| \\
\overline{e}_{\tau_n}^{[5]} &= \left|v_{\tau_n}^{1,2} - \overline{v}_{\tau_n}^{1,2}\right| \quad \text{and} \quad \widehat{e}_{\tau_n}^{[5]} = \left|v_{\tau_n}^{1,2} - \widehat{v}_{\tau_n}^{1,2}\right|
\end{aligned}$$

were evaluated. Here, for computing $X_{\tau_n}^{\{i\}}$, the realization of the Wiener process $(W_{\tau_n}^1, W_{\tau_n}^2)$ was simulated as $W_{\tau_n}^k = \sum_{j=1}^n \xi_{\tau_j}^k$, where $\xi_{\tau_j}^k$ is a realization of a Gaussian random variable with zero mean and variance Δ for each $k = 1, 2, j = 1, \ldots, n$ and $n = 1, \ldots, N$.

Fig. 1 shows the exact values of m_{τ_n}, v_{τ_n} versus their approximations $\widehat{m}_{\tau_n}, \widehat{v}_{\tau_n}$ obtained from $M = 2^{16}$ simulations of Scheme 1. Observe that there is not visual difference among these values. Table 1 presents the errors $\widehat{e}^{[l]} = \max_n\{\widehat{e}_{\tau_n}^{[l]}\}$ and $\overline{e}^{[l]} = \max_n\{\overline{e}_{\tau_n}^{[l]}\}$ of the estimated value of the mean and variance of (34) computed with different number of simulations M. As it was expected, these errors decrease as the number of simulations M increases. It is well known that the error e of the sampling mean of the Monte Carlo method decreases with the inverse of the square root of the number of simulations [11], i.e.,

$$e \propto \frac{1}{M^\gamma}$$

with $\gamma = 0.5$. A rough estimator $\gamma_{\tau_n}^{[l]}$ of γ for the errors $\widehat{e}_{\tau_n}^{[l]}$ and $\overline{e}_{\tau_n}^{[l]}$ was computed as minus the slope of the straight line fitted to the set of six points $\left\{(\log_2(M_k),\ \log_2(e_{\tau_n}^{[l]}(M_k))) :\ M_k = 2^k, k = 8, 10, 12, 14, 16, 18\right\}$. Table 2 shows the average

$$\widetilde{\gamma}^{[l]} = \frac{1}{N}\sum_{n=1}^{N} \gamma_{\tau_n}^{[l]}$$

for each type of error and its corresponding standard deviation

$$s^{[l]} = \sqrt{\frac{1}{N-1}\sum_{n=1}^{N} (\gamma_{\tau_n}^{[l]} - \gamma^{[l]})^2}.$$

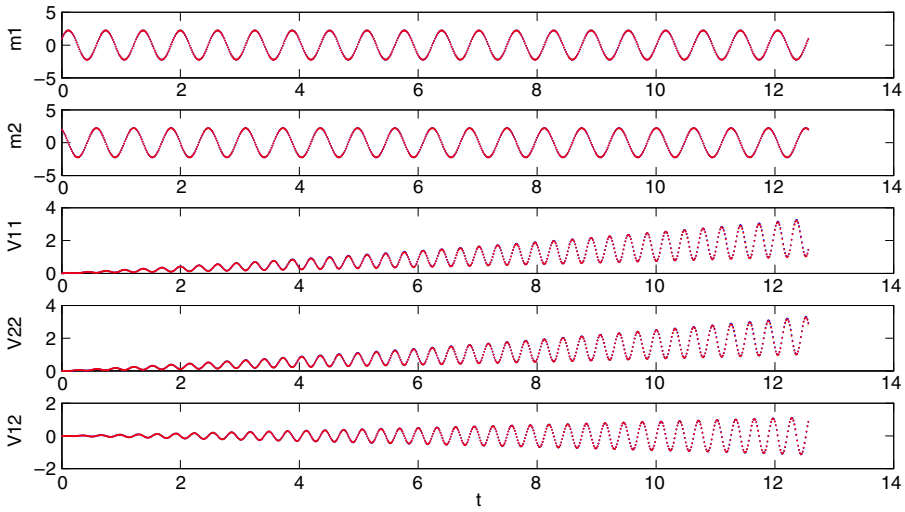

Fig. 1. Integration of Example 1. Exact values of m_{t_n}, v_{t_n} (blue) and their approximations $\widehat{m}_{t_n}$, $\widehat{v}_{t_n}$ (red) computed via Monte Carlo with $M = 2^{16}$ realizations of Scheme 1 and $\Delta = 2^{-6}$. (For interpretation of the references to color in this figure legend, the reader is referred to the web version of this article.)

Table 1
Values of the errors $\widehat{e}^{[l]}$ and $\overline{e}^{[l]}$ versus number of simulations M in Example 1.

$/M$	2^8	2^{10}	2^{12}	2^{14}	2^{16}	2^{18}
$\widehat{e}^{[1]}$	0.10710	0.05228	0.04536	0.01508	0.00686	0.00275
$\widehat{e}^{[2]}$	0.10643	0.05025	0.04469	0.01433	0.00647	0.00304
$\widehat{e}^{[3]}$	0.43411	0.25916	0.18319	0.29184	0.07244	0.03181
$\widehat{e}^{[4]}$	0.39102	0.29529	0.21413	0.29496	0.07726	0.02753
$\widehat{e}^{[5]}$	0.23859	0.14325	0.15463	0.16961	0.05187	0.02450
$\overline{e}^{[1]}$	0.27037	0.02964	0.02101	0.02108	0.01487	0.00376
$\overline{e}^{[2]}$	0.27626	0.04147	0.02327	0.02227	0.01452	0.00347
$\overline{e}^{[3]}$	0.92465	0.35064	0.18339	0.15513	0.06024	0.02482
$\overline{e}^{[4]}$	0.89503	0.39518	0.17646	0.14678	0.05655	0.02346
$\overline{e}^{[5]}$	0.36642	0.24892	0.10664	0.08899	0.02785	0.01101

Table 2
Average $\widetilde{\gamma}$ and standard deviation *std* of the estimators for the rate of convergence $\gamma = 1/2$ of the Monte Carlo simulations in Example 1.

	$\widehat{e}^{[1]}$	$\widehat{e}^{[2]}$	$\widehat{e}^{[3]}$	$\widehat{e}^{[4]}$	$\widehat{e}^{[5]}$	$\overline{e}^{[1]}$	$\overline{e}^{[2]}$	$\overline{e}^{[3]}$	$\overline{e}^{[4]}$	$\overline{e}^{[5]}$
$\widetilde{\gamma}$	0.52	0.53	0.44	0.44	0.41	0.44	0.44	0.44	0.43	0.45
std	0.16	0.16	0.20	0.20	0.21	0.18	0.19	0.21	0.21	0.20

Results of Tables 1 and 2, together with Fig. 1, indicate that the estimators for the mean and variance of (34) obtained by means of the simulations of the exact solution (35) and Scheme 1 are quite similar. This is a predictable result since the first two moments of the linear SDEs and Scheme 1 are "equal" (up to the precision of the floating-point arithmetic in the numerical computation of the involved exponential and square root matrices).

In addition, let us compute the maximum relative difference

$$r^{[l]}(M) = 100 \max_n \left\{ \left| (\overline{h}^{[l]}_{\tau_n} - \widehat{h}^{[l]}_n)/\overline{h}^{[l]}_{\tau_n} \right| \right\}$$

between the approximations

$$\overline{h}^{[l]}_{\tau_n} = \frac{1}{M}\sum_{i=1}^{M} \arctan\left(1 + \left(\left(X^l_{\tau_n}\right)^{\{i\}}\right)^2\right) \quad \text{and} \quad \widehat{h}^{[l]}_n = \frac{1}{M}\sum_{i=1}^{M} \arctan\left(1 + \left(\left(z^l_n\right)^{\{i\}}\right)^2\right)$$

of the nonlinear functionals $h^{[l]}_{\tau_n} = \mathbb{E}\left(\arctan\left(1 + (X^l_{\tau_n})^2\right)\right)$, with $l = 1, 2$. Table 3 lists the values of $r^{[l]}$ for different values of M. Observe that $r^{[l]}$ decreases as the number of simulations M increases. Furthermore, Table 3 shows that there is no significant difference between the estimates obtained from sampling the exact solution X_{τ_n} and Scheme 1, even though $\mathbb{E}\left(\arctan\left(1 + (X^l_{\tau_n})^2\right)\right)$ involves the computation of high order moments of X_{τ_n}.

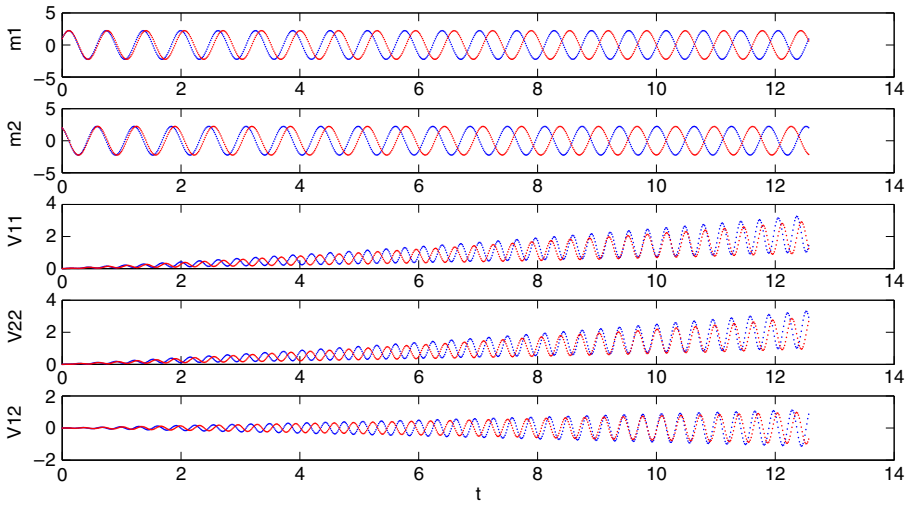

Fig. 2. Integration of Example 1. Exact values of m_{t_n}, v_{t_n} (blue) and their approximations $\widehat{m}_{t_n}$, $\widehat{v}_{t_n}$ (red) computed via Monte Carlo with $M = 2^{16}$ realizations of the Balanced scheme and $\Delta = 2^{-6}$. (For interpretation of the references to color in this figure legend, the reader is referred to the web version of this article.)

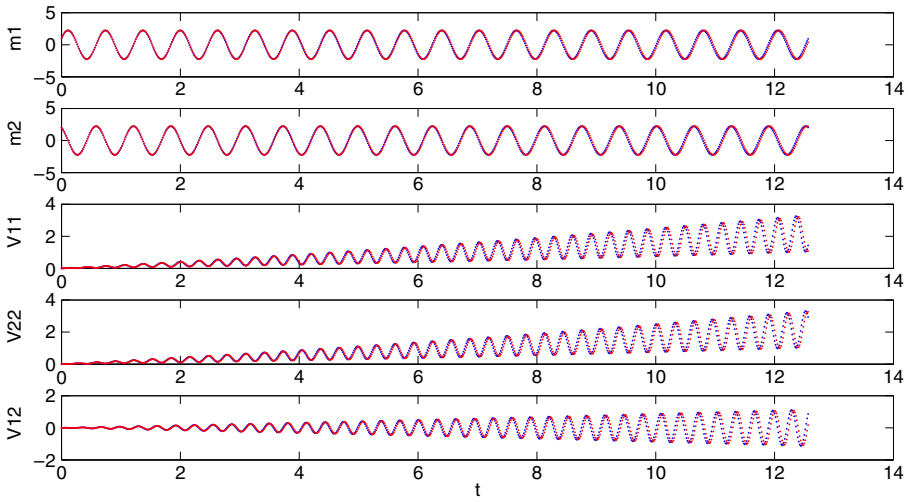

Fig. 3. Integration of Example 1. Exact values of m_{t_n}, v_{t_n} (blue) and their approximations $\widehat{m}_{t_n}$, $\widehat{v}_{t_n}$ (red) computed via Monte Carlo with $M = 2^{16}$ realizations of the Trapezoidal method and $\Delta = 2^{-6}$. (For interpretation of the references to color in this figure legend, the reader is referred to the web version of this article.)

Table 3

Maximum relative error $r^{[l]}$ in the computation of the functionals $\overline{h}^{[l]}_{\tau_n}$ and $\widehat{h}^{[l]}_n$ with different number of simulations M in Example 1.

$/M$	2^8	2^{10}	2^{12}	2^{14}	2^{16}	2^{18}
$r^{[1]}$	5.22	1.77	1.05	0.37	0.16	0.10
$r^{[2]}$	5.34	1.59	1.06	0.37	0.14	0.10

The above simulation results illustrate the feasibility of Scheme 1 for approximating functionals of linear SDEs with multiplicative noise.

At this point is worth to mention that, with the uniform time partition considered here, the Euler scheme leads to divergent results or computer overflows in the integration of Eq. (34). This contrasts with the results obtained by the Balanced and Trapezoidal methods mentioned above. Figs. 2 and 3 show, respectively, the exact values of m_{τ_n}, v_{τ_n} versus their approximations $\widehat{m}_{\tau_n}$, $\widehat{v}_{\tau_n}$ obtained from $M = 2^{16}$ simulations of the Balanced and Trapezoidal methods on the same uniform time partition considered for Scheme 1. Note that, when the time increases, the Balanced method looses the amplitude, frequency and phase of the "exact" oscillations, whereas the Trapezoidal method displays a slightly shift in

Table 4
Relative error $r_T^{[l]}$ in the computation of the functionals $\overline{h}_T^{[l]}$ and $\widehat{h}_N^{[l]}$ with different number of simulations M in Example 1.

Method	M											
	$r_T^{[1]}$						$r_T^{[2]}$					
	2^8	2^{10}	2^{12}	2^{14}	2^{16}	2^{18}	2^8	2^{10}	2^{12}	2^{14}	2^{16}	2^{18}
Balanced	7.01	5.46	4.92	4.93	4.76	4.86	2.88	2.00	2.20	2.33	2.36	2.25
Trapezoidal	5.90	7.21	6.37	6.89	6.89	7.01	2.17	1.84	2.08	2.15	2.14	2.01
Scheme 1	5.22	0.47	0.24	0.12	0.07	0.04	3.14	0.69	0.25	0.11	0.04	0.03

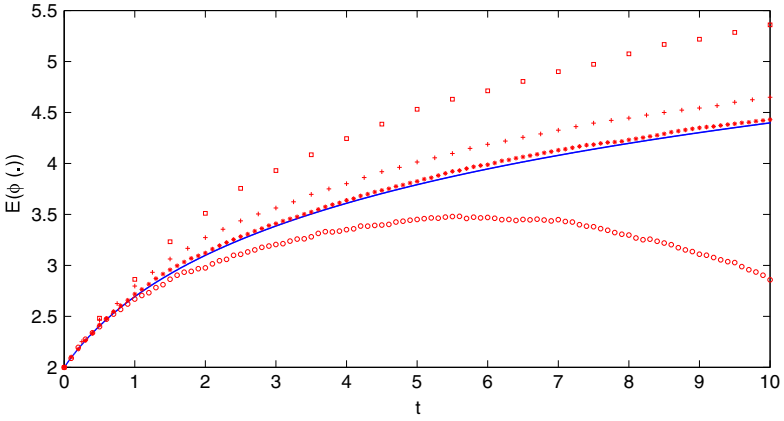

Fig. 4. Integration of Example 2. Exact Value: solid line. Euler–Romberg extrapolation method (10 000 simulations): o with $\Delta = (0.05, 0.1)$. Scheme 1 (10 000 simulations): □ with $\Delta = 0.5$, + with $\Delta = 0.25$, ∗ with $\Delta = 0.1$.

phase. This difference between schemes is more evident in Table 4, which presents the relative difference $r_T^{[l]}(M) = 100\left|(\overline{h}_T^{[l]} - \widehat{h}_N^{[l]})/\overline{h}_T^{[l]}\right|$ between the approximations $\overline{h}_T^{[l]}$ and $\widehat{h}_N^{[l]}$ to the nonlinear functional $h_T^{[l]} = \mathbb{E}\left(\arctan\left(1 + (X_T^l)^2\right)\right)$ for different values of M, where $\widehat{h}_N^{[l]}$ is now computed for each scheme. Observe that, contrary to Scheme 1, the accuracy of the Balanced and Trapezoidal methods does not improve as the number of simulations increases. This means that a reduction of the maximum stepsize Δ is required for improving the precision of these two methods.

Example 2 (*Nonautonomous Nonlinear SDE [23]*)**.**

$$d\begin{bmatrix} X_t^1 \\ X_t^2 \end{bmatrix} = \begin{bmatrix} -X_t^2 \\ X_t^1 \end{bmatrix} dt + \begin{bmatrix} 0 \\ \dfrac{\sin(X_t^1 + X_t^2)}{\sqrt{1+t}} \end{bmatrix} dW_t^1 + \begin{bmatrix} \dfrac{\cos(X_t^1 + X_t^2)}{\sqrt{1+t}} \\ 0 \end{bmatrix} dW_t^2, \tag{38}$$

with initial condition $(X_0^1, X_0^2) = (1, 1)$ and $t \in [0, 10]$. For this equation, $E(\phi(X_t)) = \left|X_{t_0}\right|^2 + \log(1+t)$, with $\phi(X) = |X|^2$.

It is well-known from [23] that via Monte Carlo simulations: (1) both, the Euler and the Milstein schemes with fixed stepsize $\Delta = 0.01$ fail to approximate $E(\phi(X_t))$; and (2) the second order Euler–Romberg extrapolation method with stepsizes 0.02 and 0.01 gives a satisfactory approximation to $E(\phi(X_t))$, but fails when the stepsizes are 0.05 and 0.1. Similarly to the fourth figure in [23], Fig. 4 illustrates this last result for a Monte Carlo estimation with $M = 10\,000$ simulations.

Fig. 4 also shows the computation of $E(\phi(X_t))$ via Monte Carlo method and Scheme 1, but on uniform time partitions with stepsizes $\Delta = 0.5, 0.25, 0.1$ and $M = 10\,000$ simulations.

In addition, Table 5 provides the estimates $\widehat{e}_N$ of the mean errors $e_N = E(\phi(z_N)) - E(\phi(X_T))$ resulting from the integration of (38) via Scheme 1 with different stepsizes. For this, the simulated realizations $z_N^{\{i,j\}}$, $i = 1, \ldots, K$ and $j = 1, \ldots, M$, were arranged into $K = 100$ batches of $M = 10\,000$ realizations each for computing

$$\widehat{e}_N = \frac{1}{K}\sum_{j=1}^{K} \widehat{e}_N^j \quad \text{with } \widehat{e}_N^j = \frac{1}{M}\sum_{i=1}^{M} \phi\left(z_N^{\{i,j\}}\right) - E\left(\phi\left(X_T\right)\right).$$

The $90\% = 100(1-\alpha)\%$ confidence interval of the Student's t distribution with $K-1$ degrees for the mean error is given by

$$[\widehat{e}_N - \Delta\widehat{e}_N, \widehat{e}_N + \Delta\widehat{e}_N],$$

where

$$\Delta\widehat{e}_N = t_{1-\alpha,K-1}\sqrt{\frac{\widehat{\sigma}_e^2}{K}}, \quad \text{with } \widehat{\sigma}_e^2 = \frac{1}{K-1}\sum_{j=1}^{K}(\widehat{e}_N^j - \widehat{e}_N)^2.$$

Table 5
Estimate $\widehat{e}_N$ of the mean error $E(\phi(z_N)) - E(\phi(X_T))$ in the integration of (38) with various stepsizes Δ.

Method	Δ				
	0.5	0.25	0.1	0.075	0.05
Euler	-256.713 ± 17.427	-33.792 ± 3.526	-5.995 ± 0.913	-3.945 ± 0.835	-2.322 ± 0.648
Balanced	-0.370 ± 0.483	0.135 ± 0.269	0.269 ± 0.249	0.241 ± 0.251	0.254 ± 0.357
Scheme 1	-0.970 ± 0.772	-0.279 ± 0.481	-0.072 ± 0.465	-0.045 ± 0.469	-0.025 ± 0.444
Trapezoidal	-0.081 ± 0.424	-0.060 ± 0.442	-0.047 ± 0.423	-0.027 ± 0.501	-0.015 ± 0.481

Table 6
Estimate of the error $\max_n \left|E(\phi(z_n)) - E(\phi(X_{t_n}))\right|$ in the integration of (38) with various stepsizes Δ.

Method	Δ								
	0.5	0.25	0.1	0.075	0.05	0.025	0.01	0.0075	0.005
Euler	256.713	33.792	5.995	3.945	2.322	1.034	0.384	0.282	0.192
Balanced	1.070	0.703	0.396	0.355	0.278	0.196	0.144	0.136	0.110
Scheme 1	0.970	0.279	0.072	0.045	0.025	0.014	0.009	0.007	0.006
Trapezoidal	0.111	0.084	0.047	0.030	0.017	0.015	0.008	0.004	0.004

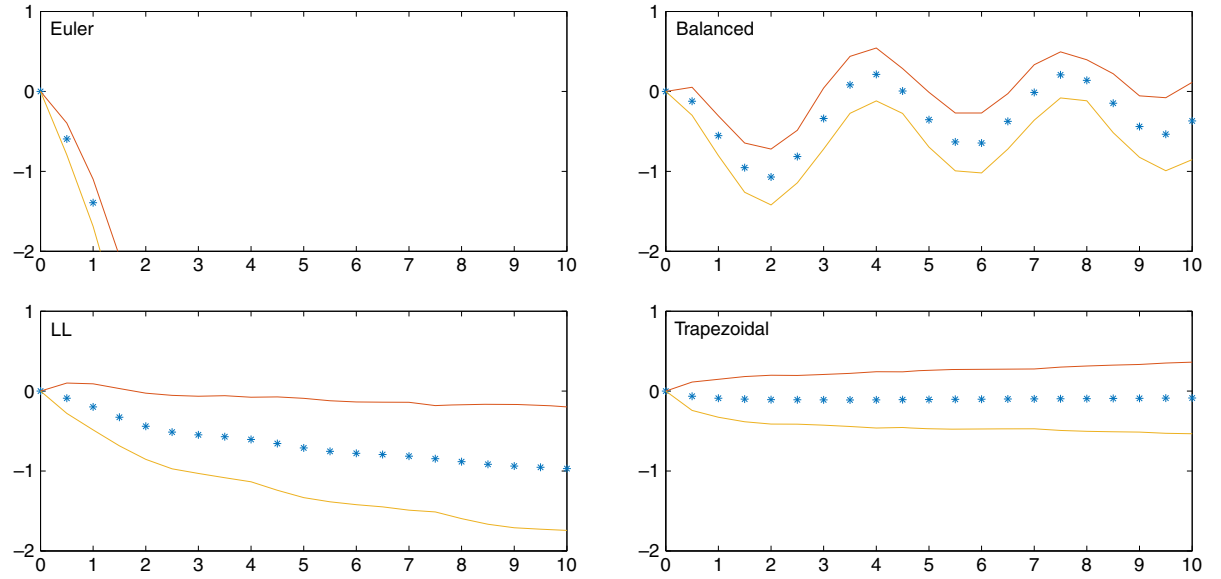

Fig. 5. Integration of Example 2. Dots: Estimates $\widehat{e}_n$ of the mean errors $e_n = E(\phi(z_n)) - E(\phi(X_{t_n}))$ resulting from the integration of (38) via the Euler, Scheme 1 (LL), Balanced and Trapezoidal methods with $\Delta = 0.5$. Solid lines: 90% confidential interval $[\widehat{e}_n - \Delta\widehat{e}_n, \widehat{e}_n + \Delta\widehat{e}_n]$.

For comparison, the same estimate of the mean error for the Euler, Balanced and Trapezoidal methods is also given in Table 5. However, a much better picture about the performance of each integrator is given in Figs. 5–7, and in Table 6. Each figure gives the estimates $\widehat{e}_n$ of the mean errors $e_n = E(\phi(z_n)) - E(\phi(X_{\tau_n}))$ resulting from the integration of (38) via Scheme 1, Euler, Balanced and Trapezoidal methods with different stepsizes Δ, for all $\tau_n = n\Delta$ and $n = 0, \ldots, N$, where $\widehat{e}_n$ is calculated as $\widehat{e}_N$ in the previous paragraph. Table 6 lists the values of $\max_n |\widehat{e}_n|$ corresponding to each one of these methods for the same stepsizes of Table 5 and smaller. Clearly, for the biggest stepsize $\Delta = 0.5$, the accuracy of the Trapezoidal method is the best, followed by that of Scheme 1, the Balanced and the Euler schemes. For the middle and smallest stepsizes $\Delta = 0.05$ and $\Delta = 0.005$, respectively, there is not significative difference between the accuracy of Trapezoidal method and Scheme 1 in comparison with the much lower precision of the other two integrators.

With regard to the computational time, Table 7 presents the relative CPU time spent for these schemes per realization, which is obtained as the ratio of the actual CPU time for each scheme to the minimum of all CPU times. Clearly, there is a substantial difference between the computational cost of these schemes. This is so due to two main factors: (1) the different complexity level of the algorithms involved in each scheme; and (2) the computational efficiency of the code that implements these algorithms. Whereas the Euler method only needs a random number generator algorithm and the evaluation of the drift and diffusion coefficients at each integration step, the remainder schemes require of other time consuming algorithms as those for the solution of linear and nonlinear algebraic equations, and the computation of matrix exponential and square root. We recall here that Matlab2014a provides fast "building in code" for the solution of linear equations and much slower "Matlab code" for the other mentioned algorithms, which certainly favors the computational

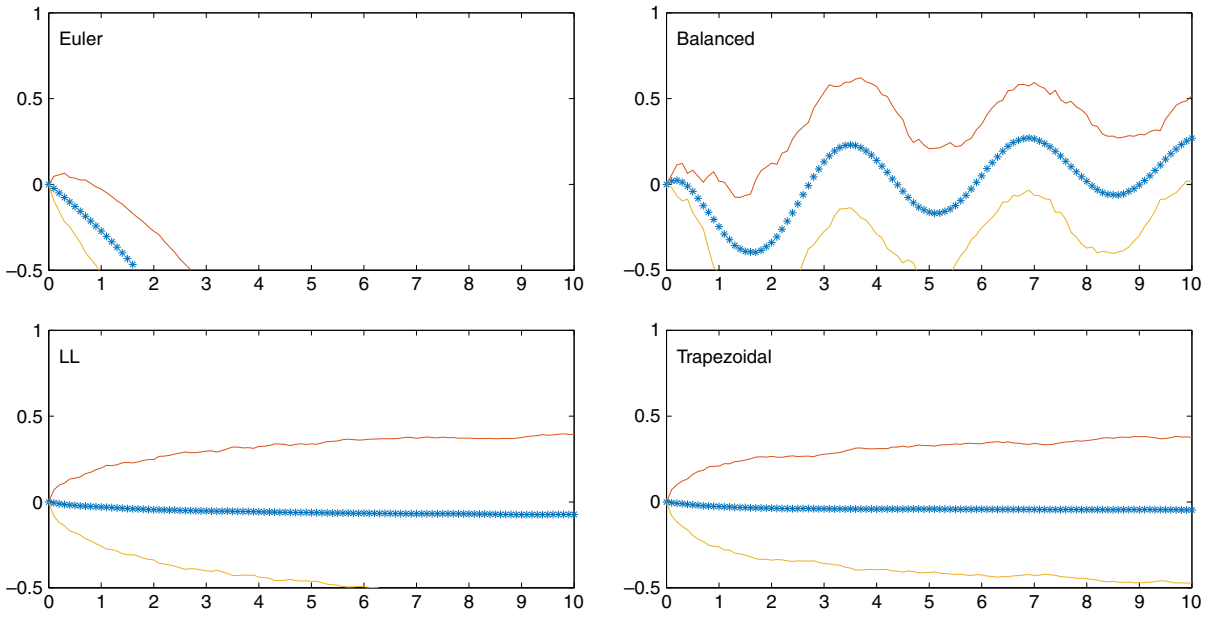

Fig. 6. Integration of Example 2. Dots: Estimates $\widehat{e}_n$ of the mean errors $e_n = E(\phi(z_n)) - E(\phi(X_{t_n}))$ resulting from the integration of (38) via the Euler, Scheme 1 (LL), Balanced and Trapezoidal methods with $\Delta = 0.1$. Solid lines: 90% confidential interval $[\widehat{e}_n - \Delta\widehat{e}_n, \widehat{e}_n + \Delta\widehat{e}_n]$.

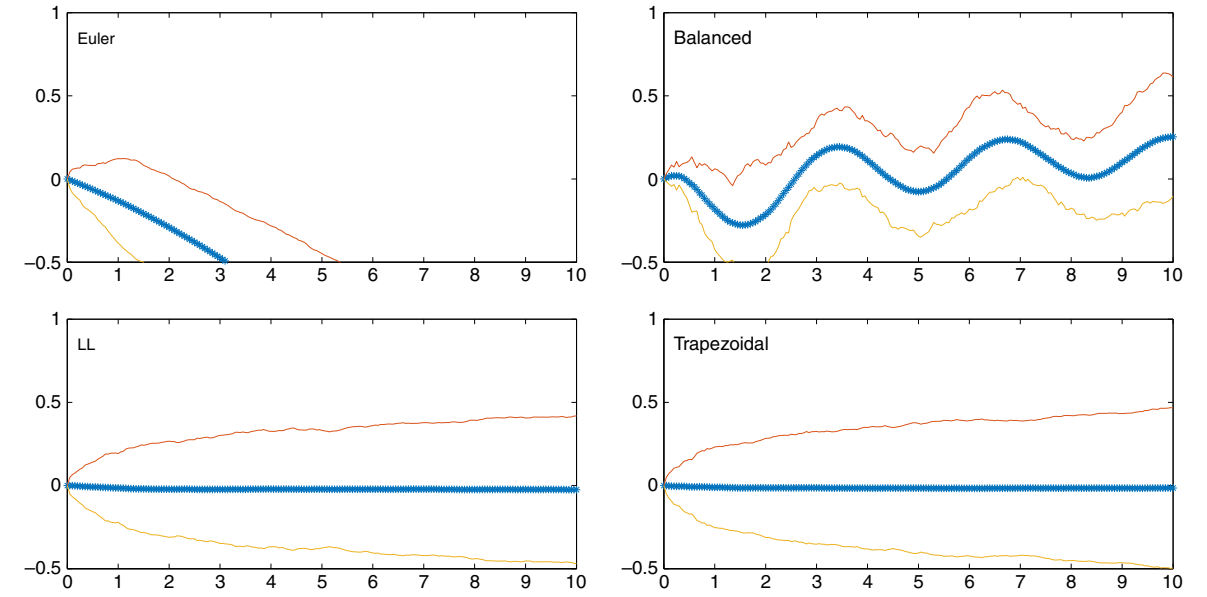

Fig. 7. Integration of Example 2. Dots: Estimates $\widehat{e}_n$ of the mean errors $e_n = E(\phi(z_n)) - E(\phi(X_{t_n}))$ resulting from the integration of (38) via the Euler, Scheme 1 (LL), Balanced and Trapezoidal methods with $\Delta = 0.05$. Solid lines: 90% confidential interval $[\widehat{e}_n - \Delta\widehat{e}_n, \widehat{e}_n + \Delta\widehat{e}_n]$.

Table 7
Relative CPU times between the different numerical schemes for various stepsizes Δ.

Method	Δ								
	0.5	0.25	0.1	0.075	0.05	0.025	0.01	0.0075	0.005
Euler	1.0	2.0	4.5	8.7	12.9	19.7	51.3	79.9	118.9
Balanced	3.3	8.0	17.5	30.5	44.2	66.5	191.1	255.3	408.7
Scheme 1	29.9	71.1	149.8	302.9	395.8	643.4	1719.5	2438.4	4221.2
Trapezoidal	138.4	306.7	610.0	1178.1	1563.3	2133.6	6130.2	8248.0	13000.5

efficiency of the Balanced method over that of the Trapezoidal method and Scheme 1. Thus, the relative CPU time difference between these three integrators in Table 7 should be thought as a maximum gap that can be sensible reduced with implementations of the Trapezoidal method and Scheme 1 that also include "building in code" for the implicated complex algorithms. In particular, for Scheme 1 applied to low dimensional SDEs additional reduction of the computational cost can be archived with implementations involving simpler matrix square root algorithms and low order Padé methods as those considered in [25,26]. For middle and high dimensional systems of SDEs, Scheme 1 might not be particularly appropriate since the computational cost most likely grows faster with the size of the system. In this situation, implementations involving Krylov subspace methods for computing the exponential and square root of matrices will be particularly necessary for reducing the computational budget of Scheme 1.

6. Conclusions

A weak Local Linearization scheme for stochastic differential equations with multiplicative noise was introduced. The scheme preserves the first two moments of the solution of linear SDEs and the mean-square stability and instability that such solution may have. The order-1 of weak convergence was proved and the practical performance of the scheme in the evaluation of functionals of linear and nonlinear test equations was illustrated with numerical simulations. For the linear test equation, the simulations showed significant higher accuracy of the introduced scheme in comparison with the Euler, Balanced and Trapezoidal methods. For the nonlinear test equation, the accuracy of the Local Linearization scheme was similar to the best obtained by the Trapezoidal method, but with lower computational time, and it was higher than that of the other two integrators with the same stepsize.

Acknowledgments

This work was partially supported by the FONDECYT Grant 1140411. The second author also thanks the funding of the BASAL Grant PFB-03.

References

[1] R. Biscay, J.C. Jimenez, J. Riera, P. Valdes, Local linearization method for the numerical solution of stochastic differential equations, Ann. Inst. Statist. Math. 48 (1996) 631–644.
[2] C. Mora, Numerical solution of conservative finite-dimensional stochastic Schrödinger equations, Ann. Appl. Probab. 15 (2005) 2144–2171.
[3] I. Shoji, A note on convergence rate of a linearization method for the discretization of stochastic differential equations, Commun. Nonlinear Sci. Numer. Simul. 16 (2011) 2667–2671.
[4] O. Stramer, The local linearization scheme for nonlinear diffusion models with discontinuous coefficients, Statist. Probab. Lett. 42 (1999) 249–256.
[5] J.C. Jimenez, R. Biscay, Approximation of continuous time stochastic processes by the Local Linearization method revisited, Stoch. Anal. Appl. 20 (2002) 105–121.
[6] J.C. Jimenez, F. Carbonell, Rate of convergence of local linearization schemes for initial-value problems, Appl. Math. Comput. 171 (2005) 1282–1295.
[7] J.C. Jimenez, T. Ozaki, Local Linearization filters for nonlinear continuous-discrete state space models with multiplicative noise, Internat. J. Control 76 (2003) 1159–1170.
[8] F. Carbonell, J.C. Jimenez, R.J. Biscay, Weak local linear discretizations for stochastic differential equations: convergence and numerical schemes, J. Comput. Appl. Math. 197 (2006) 578–596.
[9] J.C. Jimenez, Simplified formulas for the mean and variance of linear stochastic differential equations, Appl. Math. Lett. 49 (2015) 12–19.
[10] J.C. Jimenez, T. Ozaki, Linear estimation of continuous-discrete linear state space models with multiplicative noise, Systems Control Lett. 47 (2002) 91–101.
[11] P.E. Kloeden, E. Platen, Numerical Solution of Stochastic Differential Equations, second ed., Springer-Verlag, Berlin, 1995.
[12] G.N. Milstein, M.V. Tretyakov, Stochastic Numerics for Mathematical Physics, Springer, 2004.
[13] M. Gitterman, The Noisy Oscillator, World Scientific, 2005.
[14] A. Robler, M. Seaid, M. Zahri, Method of lines for stochastic boundary-value problems with additive noise, Appl. Math. Comput. 199 (2008) 301–314.
[15] D.J. Higham, Mean-square and asymptotic stability of the stochastic Theta method, SIAM J. Numer. Anal. 38 (2000) 753–769.
[16] C. Moler, C. Van Loan, Nineteen dubious ways to compute the exponential of a matrix, twenty-five years later, SIAM Rev. 45 (2003) 3–49.
[17] Y.S. Chow, H. Teicher, Probability Theory: Independence, Interchangeability, Martingales, Springer, 2012.
[18] J.C. Jimenez, R. Biscay, C. Mora, L.M. Rodriguez, Dynamic properties of the Local Linearization method for initial-value problems, Appl. Math. Comput. 126 (2002) 63–81.
[19] G. Milstein, M. Tretyakov, Numerical methods in the weak sense for stochastic differential equations with small noise, SIAM J. Numer. Anal. 34 (1997) 2142–2167.
[20] G.H. Golub, C.F. Van Loan, Matrix Computations, third ed., The Johns Hopkins University Press, 1996.
[21] Y. Saito, T. Mitsui, Stability analysis of numerical schemes for stochastic differential equations, SIAM J. Numer. Anal. 33 (1996) 2254–2267.
[22] H. Schurz, Convergence and stability of balanced implicit methods for systems of SDEs, Int. J. Numer. Anal. Model. 2 (2005) 197–220.
[23] D. Talay, L. Tubaro, Expansion of the global error for numerical schemes solving stochastic differential equations, Stoch. Anal. Appl. 8 (1990) 94–120.
[24] L. Arnold, Stochastic Differential Equations: Theory and Applications, Wiley-Interscience Publications, New York, 1974.
[25] N.J. Higham, Computing real square roots of a real matrix, Linear Algebra Appl. 88/89 (1987) 405–430.
[26] J.C. Jimenez, F. Carbonell, Convergence rate of weak Local Linearization schemes for stochastic differential equations with additive noise, J. Comput. Appl. Math. 279 (2015) 106–122.